Journal of Colloid and Interface Science 584 (2021) 34–44

Contents lists available at ScienceDirect

Journal of Colloid and Interface Science

journal homepage: www.elsevier.com/locate/jcis

Regular Article

Effective cytocompatible nanovectors based on serine-derived gemini surfactants and monoolein for small interfering RNA delivery

Catarina Costa [a,b,c], Isabel S. Oliveira [a], João P.N. Silva [a], Sandra G. Silva [d], Cláudia Botelho [b,e], M. Luísa C. do Vale [d], Maria Elisabete C.D. Real Oliveira [c], Andreia C. Gomes [b,*], Eduardo F. Marques [a,*]

[a] CIQUP, Departamento de Química e Bioquímica, Faculdade de Ciências, Universidade do Porto, Rua do Campo Alegre s/n, 4169-007 Porto, Portugal
[b] CBMA (Centro de Biologia Molecular e Ambiental), Departamento de Biologia, Campus de Gualtar, Universidade do Minho, 4710-057 Braga, Portugal
[c] CF-UM-UP, Departamento de Física, Campus de Gualtar, Universidade do Minho, 4710-057 Braga, Portugal
[d] LAQV-REQUIMTE, Departamento de Química e Bioquímica, Faculdade de Ciências, Universidade do Porto, Rua do Campo Alegre s/n, 4169-007 Porto, Portugal
[e] CEB (Centro de Engenharia Biológica), Departamento de Engenharia Biológica, Campus de Gualtar, Universidade do Minho, 4710-057 Braga, Portugal

GRAPHICAL ABSTRACT

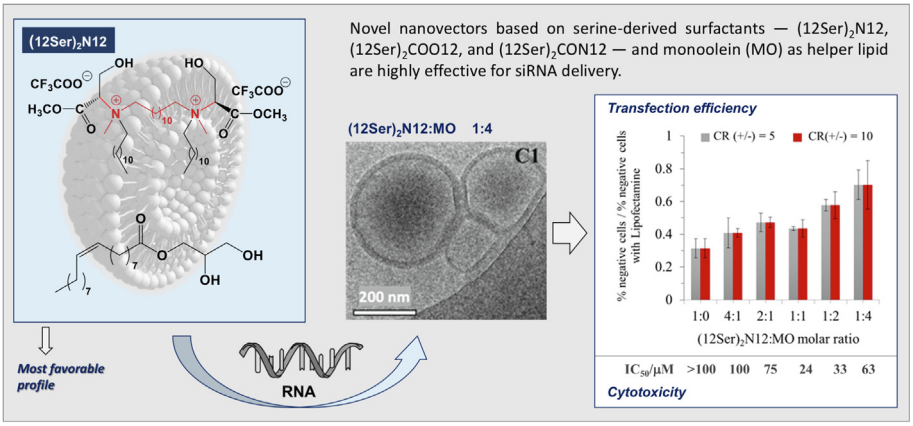

ARTICLE INFO

Article history:
Received 25 June 2020
Revised 19 August 2020
Accepted 20 September 2020
Available online 25 September 2020

Keywords:
Gemini surfactant
Serine
siRNA-delivery
Lipoplex properties
Monoolein helper lipid
Transfection efficiency

ABSTRACT

Non-viral gene therapy based on gene silencing with small interfering RNA (siRNA) has attracted great interest over recent years. Among various types of cationic complexation agents, amino acid-based surfactants have been recently explored for nucleic acid delivery due to their low toxicity and high biocompatibility. Monoolein (MO), in turn, has been used as helper lipid in liposomal systems due to its ability to form inverted nonbilayer structures that enhance fusogenicity, thus contributing to higher transfection efficiency. In this work, we focused on the development of nanovectors for siRNA delivery based on three gemini amino acid-based surfactants derived from serine — $(12Ser)_2N12$, amine derivative; $(12Ser)_2COO12$, ester derivative; and $(12Ser)_2CON12$, amide derivative — individually combined with MO as helper lipid. The inclusion of MO in the cationic surfactant system influences the morphology and size of the mixed aggregates. Furthermore, the gemini surfactant:MO systems showed the ability to efficiently complex siRNA, forming stable lipoplexes, in some cases clearly depending on the MO content, without inducing significant levels of cytotoxicity. High levels of gene silencing were achieved in

* Corresponding authors.
E-mail addresses: agomes@bio.uminho.pt (A.C. Gomes), efmarque@fc.up.pt (E.F. Marques).

https://doi.org/10.1016/j.jcis.2020.09.077

comparison with a commercially available standard indicating that these gemini:MO systems are promising candidates as lipofection vectors for RNA interference (RNAi)-based therapies.

1. Introduction

The fast development of nanoscience and nanotechnology over the last decade has prompted the emergence of robust and effective nucleic acid delivery systems for gene therapy to prospectively replace viral vectors [1–3]. The discovery of RNA interference (RNAi), and subsequent findings of its mechanisms of action, opened up exciting possibilities for its use in gene therapy, and generated new perspectives for hard-to-treat diseases [4–6]. Small RNAs are introduced into human, animal or plant cells, and activate the RNA interference machinery to break down mRNA with a complementary sequence. However, a major challenge to the use of RNAi-based therapies is their efficient delivery through an appropriate vector to avoid rapid elimination by endogenous nucleases [7–10]. Over the last years, much work has focused on the development of effective vectors for small interfering RNA (siRNA) delivery, particularly liposomes and other types of colloidal nanocarriers [11–15].

Gemini or dimeric surfactants, with two polar heads and two hydrocarbon tails per molecule separated by a spacer group connected at the level of the headgroups, have been subject of great attention, both from fundamental [16,17] and application-oriented perspectives [18,19]. This continuous interest results from their unique physicochemical properties, which can be modified by adjusting their structural elements, namely the polar headgroups, hydrocarbon tails and covalent spacer [20–22]. Cationic gemini surfactants, in particular, have been employed with the goal of attaining more effectiveness for gene delivery [23–33]. Most reports have focused on compounds with quaternary ammonium headgroups and linear aliphatic tails, called bis-quats [31,33]. However, these surfactants exhibit relatively high levels of cytotoxicity, which limit their use in biomedical applications [34]. To overcome this problem, gemini surfactants based on natural structural motifs such as sugars, amino acids and peptides have been designed and synthesized [6,35–37]. These compounds combine the efficiency of the gemini molecular structure with the biocompatibility of biomacromolecules, hence presenting enhanced physico-chemical and biological profiles [38,39]. Several studies have shown that the introduction of amino acid motifs in the structure of gemini amphiphiles promotes an increase in transfection efficiency compared to conventional standards such as Lipofectamine [23,40–42].

Previous work by our group on the synthesis and characterization of amino acid-derived single-tailed surfactants derived from serine, tyrosine and 4-hydroxyproline has shown that the optimal toxicological profile and most interesting physicochemical properties are obtained with the serine derivatives [43–45]. These results lead us to the synthesis of cationic serine-based gemini surfactants, exploring the multifunctionality of the serine headgroup, by changing the spacer chain length as well as the nature of the bond linking the spacer to the amino acid residue (as can be seen in Fig. 1A–C) [46]. These novel surfactants displayed enhanced interfacial properties relative to homologous bis-quats [40,46,47], thus allowing the use of lower amounts of compound to achieve the same therapeutic effect, which is of particular interest for biomedical applications [48].

The inclusion of helper lipids in liposomal formulations is one of the possible strategies to potentiate transfection efficiency of cationic surfactants by improving both the system's stability in physiological conditions and the endosomal escape ability [49,50]. Recently, monoolein (MO) has been used as an efficient helper lipid in liposomal systems for plasmidic DNA (pDNA) and siRNA delivery [51–54]. MO is a neutral single-tailed unsaturated lipid (Fig. 1D) that is known to self-assemble in water into non-bilayer reverse structures, namely the inverted cubic phases Ia3d and Pn3m [55,56]. In mixtures, MO is not only capable to fluidize and stabilize the liposomal structures, but can also form reverse cubic or hexagonal phases [11,57], known to enhance fusogenicity, thus contributing to a higher transfection efficiency of MO-containing lipoplexes [51–54].

The aim of this work was to develop nanovectors for therapeutic siRNA delivery based on serine-derived gemini surfactants combined with MO as helper lipid and to investigate the role of chemical differences in the polar headgroup. All the surfactants contain a 12-carbon alkyl chain linked to the nitrogen atom of the amino acid and a 12-carbon spacer, connecting the two monomeric entities through their headgroups. They differ in the nature of the spacer linkage, as shown in Fig. 1A to 1C; $(12Ser)_2N12$ is an amine derivative (A); $(12Ser)_2COO12$, an ester derivative (B) and $(12Ser)_2CON12$, an amide derivative (C). The amine derivative is a micelle-forming surfactant, while the ester and amide ones form bilayer structures, namely vesicles at low concentration [12]. Herein, we start by showing the cytotoxicity profiles of the gemini-MO lipoplexes as well as their ability to effectively deliver their load and silence a target gene. Given the interesting transfection results obtained, and in order to gain further insight, we then proceeded to the characterization of shape, size and charge of the mixed gemini:MO aggregates (containing varying content of the helper lipid) and of the lipoplexes formed with different gemini: RNA charge ratios, CR (+/-), in an effort to withdraw structure–activity relationships.

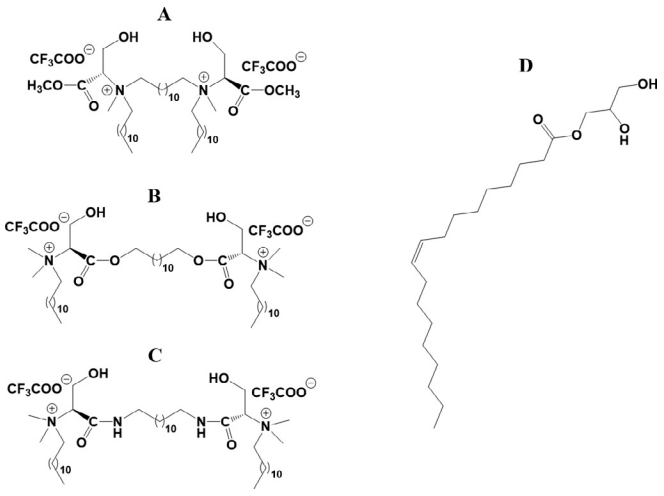

Fig. 1. Molecular structure of the amphiphiles used in this work. The gemini surfactants A-C differ on the nature and location of the linkage between spacer and serine-based headgroup: A, $(12Ser)_2N12$, amine derivative; B, $(12Ser)_2COO12$, ester derivative; and C, $(12Ser)_2CON12$, amide derivative. D is the helper lipid monoolein.

2. Experimental section

2.1. Materials

Serine derivatives *O*-*tert*-butyl L-serine, H-Ser(tBu)–OH (>99%) and *O*-*tert*-butyl L-serine methyl ester hydrochloride, H-Ser(tBu)-OMe.HCl (>99%) and the coupling agents benzotriazol-1-yloxy-tri pyrrolidino-phosphonium hexafluorophosphate (PyBOP) and *O*-(Benzotriazol-1-yl)-*N*,*N*,*N*',*N*'-tetramethyluronium tetrafluoroborate (TBTU) were purchased from Bachem. Solvents (p.a. quality) and other chemicals, including 3-(4,5-dimethyl-2-thiazolyl)-2,5-d iphenyl-2*H*-tetrazolium bromide (MTT), were obtained from Sigma-Aldrich. Thin layer chromatography (TLC) aluminum foil plates covered with silica 60 F254 (0.25 mm) and silica-gel 60 (70–230 mesh ASTM) for preparative column chromatography were from Merck and SDS, respectively. The fluorescent lipid rhodamine-phosphatidylethanolamine (λ_{exc} = 545 nm; λ_{em} = 576-nm) and the heat-inactivated fetal bovine serum (FBS) were acquired from Invitrogen. The transfection reagent Lipofectamine®RNAiMAX and the Quant-iT™ RiboGreen® RNA assay kit were obtained from Life Technologies. siRNA targeting the enhanced green fluorescent protein (sieGFP) and a siRNA negative control duplex (siCONTROL), with HPLC purification, were purchased from Integrated DNA Technologies. The compositions are: sieGFP: sense strand = 5′-CAAGCUGACCCUGAAGUUdTdT-3′; antisense strand = 5′-AACUUCAGGGUCAGCUUGdTdT-3′; siCONTROL: sense strand = 5′-(5′UGCGCUACGAUCGACGAUdTdT3′); antisense strand = 5′-AUCGUCGAUCGUAGCGCAdTdT-3′.

Monoolein (1-monooleoyl-*rac*-glycerol), 99% purity, was purchased from Sigma-Aldrich. The serine-derived surfactants shown in Fig. 1, A – dodecamethylene 1,12-bis{*N*-(dodecyl)-*N*-[(1*S*)-(2-h ydroxy-1-methyloxycarbonyl)ethyl]-*N*-(methyl)ammonium} bis (trifluoroacetate), B – *O*,*O*'-dodecane-1,12-diyl-bis{*N*-[(1*S*)-(1-oxycarbonyl-2-hydroxy)ethyl]-*N*-dodecyl-*N*,*N*-dimethyl ammonium} bis(trifluoroacetate) and C — *N*', *N*''-dodecane-1,12-diyl-bis {*N*-[(1*S*)-(1-carbamoyl-2-hydroxyethyl]-*N*-dodecyl-*N*,*N*-dimethyl ammonium} bis(trifluoroacetate), were synthesized according to a previous report [46], where details on the synthetic procedures, purification, and purity data (NMR, high resolution mass spectrometry and surface tension) are available.

2.2. Methods

2.2.1. Sample preparation

Mixtures with different gemini surfactant:MO molar ratios, namely (1:0), (4:1), (2:1), (1:1), (1:2) and (1:4), were prepared by thin lipid film hydration. Briefly, defined volumes of each serine derivative and MO stock solutions (both 20 mM in ethanol) were mixed and the solvent removed under vacuum using a rotary evaporator, at 60 °C for 45 min. The dried films were then hydrated with ultrapure (Milli-Q) water at 40 °C for 30 min, to a final amphiphile concentration of 1 mM or 5 mM.

2.2.2. Preparation of siRNA-lipoplexes

Lipoplexes were prepared at 25 °C by adding defined aliquots of 1 mM aqueous solutions of the gemini:MO mixtures (for all molar ratios studied) to 10 μL of siRNA solution (10 μg·mL^{-1}), to obtain surfactant/siRNA CRs ranging from 0.5 to 20. The surfactant-to-siRNA charge ratio, CR (+/-), is defined as:

$$CR(+/-) = \frac{2 \times [\text{gemini surfactant}]}{[\text{siRNA phosphate groups}]} \quad (1)$$

since each gemini molecule carries two positive charges. The lipoplexes were incubated at room temperature, under vortex stirring, for 30 s, and then diluted with ultrapure water to a final siRNA concentration of 10 ng·mL^{-1}. The samples were allowed to rest for one hour before use.

2.2.3. Dynamic light scattering (DLS)

The size (mean diameter, <D_H>), and zeta (ζ) potential of the aggregates formed by the neat surfactants, the gemini:MO mixtures as well as siRNA-lipoplexes were measured with a Malvern ZetaSizer Nano ZS, at 25 °C. Disposable polystyrene cuvettes for size measurements and U-shaped zeta potential cuvettes were used. Both for DLS and zeta potential measurements a minimum of 5 repeats per sample were performed. In DLS, the autocorrelation function of the scattered light was fitted with the Zetasizer Software® v7.12 using different algorithms [58,59]: for the lipoplexes, the cumulants analysis algorithm was used to obtain the mean size (*z*-average) and polydispersity index, as the samples presented a unimodal, low polydispersity distribution; for the gemini:MO aggregates, given the multimodal or polydisperse unimodal character of the distributions, a non-negative least squares (NNLS) algorithm was used. The results are presented in scattered intensity distribution data. For the zeta potential measurements, the electrophoretic mobility, μ, was measured using a combination of electrophoresis and laser Doppler velocimetry techniques, and the ζ-potential was calculated from μ using the Henry equation, with a dielectric constant of 78.5, a medium viscosity of 0.89 cP, and a f(κa) function value of 1.5 (Smoluchowsky approximation).

2.2.4. Light microscopy

Light micrographs of serine-based surfactant: MO formulations were obtained with an Olympus BX51 microscope, equipped with Differential Interface Contrast (DIC). The images were obtained with a DP71 digital video-camera and processed using the cellA software from the manufacturer.

2.2.5. Cryo-transmission electron microscopy (Cryo-TEM)

Cryo-TEM was used for microstructure studies of lipoplexes. The samples were prepared in an automatic plunge freezing from Leica (Leica EM GP). A drop of the solution was placed on TEM grids, the excess of solution was blotted to create a thin film over the grid which was rapidly plunged into liquid ethane at its freezing point. After the vitrification process, the samples were transferred, using a Gatan cryo holder, to the electron microscope, JEOL JEM-2011, and the images were recorded with a CCD GATAN 895 USC 4000 camera.

2.2.6. Cells lines and culture conditions

Human Embryonic Kidney Cells (HEK293T; ATCC, USA), wild type, or stably expressing enhanced green fluorescent protein (HEK293eGFP; ECACC, UK) were grown in Dulbecco's minimal essential medium (DMEM), supplemented with 10% heat inactivated fetal bovine serum (FBS), 1% penicillin–streptomycin, 1% L-glutamine and 1% sodium pyruvate (supplemented with 2 μg/mL puromycin) in a humidified incubator (5% CO_2, 37 °C). Cells were subcultured every 2 days using 0.05% Trypsin-EDTA solution in order to maintain subconfluency.

2.2.7. MTT cytotoxicity assay

The percentage of viable cells after incubation with gemini:MO aggregates was determined by the MTT assay, which evaluates metabolic activity. HEK293T cells were seeded into 96-well culture plates at a cell density of 1.5 × 10^4 cells per well in complete cell culture medium. Before the addition of the aggregates, the culture medium was removed and replaced by 100 μL of fresh culture medium. Defined aliquots of the testing samples (pre-sterilized by filtration through a membrane filter with a pore diameter of 450 nm; 100 μg·mL^{-1}) were then added to each well to achieve final surfactant concentrations of 10, 25, 50 and 100 μM. During

the experiments positive (cells without addition of surfactant) and negative (cells in the presence of 100 μL DMSO) controls were prepared. Cell viability was determined after 48 h according to manufacturer's instructions.

2.2.8. siRNA complexation efficiency

The complexation efficiency of siRNA was determined using the RiboGreen reagent according to the manufacturer's instructions. Briefly, 200 μL of serine-based aggregates were mixed with 100 μL of a RiboGreen solution (1:2000 in TE buffer) in a 96-well culture plate. After 5 min of incubation at room temperature, the fluorescence was measured in a Fluoroskan Ascent™ FL Microplate Fluorometer and Luminometer (Thermo scientific) using an excitation/emission filter pair of 485/538 nm.

2.2.9. eGFP silencing

The eGFP silencing was evaluated and quantified by flow cytometry. The siRNA-lipoplexes at CR (+/-) = 5 and 10 were prepared with 30 nM of siRNA eGFP-targeting siRNA (sieGFP), ensuring that all systems were above the critical aggregation concentration of the gemini:MO mixture. HEK293eGFP cells were seeded into 24-well culture plates at a cell density of 1.0×10^5 cells per well, in complete cell culture medium, and incubated overnight at 37 °C and in 5% CO_2. Then, the cell culture medium was removed and replaced by a fresh medium containing 60 μL of the siRNA-lipoplexes solution. Lipofectamine®RNAiMAX lipoplexes containing sieGFP, prepared according to procedures described by the supplier, were used as positive control.

After 48 h of incubation, cells were analyzed on an EC800 Flow Cytometry Analyzer (Sony Biotechnology Inc., Champaign, IL, USA). To exclude debris from the analysis, the discriminant was set to the forward scatter of the channel in the linear-peak mode. eGFP was excited by a diode blue laser (488 nm) and the green autofluorescence of cells expressing eGFP was detected using a 530/50 nm bandpass filter in the FL1 channel. Fluorescence signal was amplified with the logarithmic mode. A sample volume of 150 μL was analyzed at a flow rate of 60 $\mu L \cdot min^{-1}$. Total events of 15,000–25,000 cells were counted. Every sample was run in triplicate for reproducibility of the experiment. Analysis of data was performed on the EC800 software version 1.3.6. (Sony Biotechnology Inc., Champaign, IL, USA).

3. Results and discussion

3.1. Cytotoxicity of gemini/monoolein systems

The characterization of the cytotoxicity profile of novel nanovectors is particularly relevant for the development of safe biomedical nanodevices. The results for cytotoxicity studies initially performed for the gemini/MO mixtures with varying MO content can be seen in Table 1, where the IC_{50} (minimum concentration to promote 50% decrease in cell viability) values are shown (see also supplementary data, Fig. S1). Several trends can be observed. First, the inclusion of MO has different effects depending on the gemini type: for the amine, MO induces higher cytotoxicity compared to the neat surfactant, but the dependence is non-monotonic, achieving lowest IC_{50} at equimolarity (Table 1); for the ester, MO induces a moderate but steady increase in cytotoxicity; for the amide, the effect of increasing MO is practically null, with a slight decrease in cytotoxicity at high MO contents. Secondly, if we compare the systems at highest MO content (1:4 molar ratio), then the order of increasing cytotoxicity is amine < ester < amide. Thirdly and most importantly, all formulations induce low or no cytotoxicity (cell viability higher than 70% according to International Standards Organization guidelines) at concentrations below ~ 20 μM. As the physiological concentrations of surfactant/lipid mixture necessary for transfection are typically below 20 μM, it can be concluded that these vectors are not cytotoxic for the useful concentration range needed.

Table 1
The values of IC_{50} determined by MTT assay in HEK 293T cell line upon exposure to aqueous mixtures of the serine-based surfactants and MO at varying cationic surfactant/MO molar ratios. For each system, the total surfactant/MO concentration was varied between 10 and 100 μM.

	IC_{50}*/μM		
	Amine-derivative	Ester-derivative	Amide-derivative
gemini:MO molar ratio	$(12Ser)_2N12$	$(12Ser)_2COO12$	$(12Ser)_2CON12$
1:0	>100	>100	18
4:1	100	>100	18
2:1	75	39	18
1:1	24	35	18
1:2	33	34	28
1:4	63	29	21

* Typical uncertainty: ±10%.

3.2. Transfection efficiency of gemini/monoolein/siRNA systems

HEK293eGFP cells constitutively overexpress eGFP. Therefore, transfecting siRNA that silences the respective gene, expressed in high levels in these cells, offers a straightforward way to evaluate the efficacy of a novel transfection system. Commercially available Lipofectamine developed for siRNA delivery was chosen as the standard, and all the results obtained in the flow cytometry analysis are expressed in relation to this transfection control, as % of HEK293eGFP cells not expressing eGFP after 48 h incubation with the different systems (Fig. 2). CRs (+/-) of 5 and 10 were chosen for all systems (see further Section 3.4) to encapsulate 30 nM siRNA, necessary for efficient gene silencing. The total gemini/MO concentrations were maintained below 18 μM (i.e. below the IC_{50} of any mixture, Table 1).

The data presented in Fig. 2 reveal striking differences in transfection efficiency depending on the content of MO and, in two of the systems, on the CR (+/-). A clear trend is that lipoplexes with MO generally lead to better eGFP gene silencing efficiency compared to those with gemini surfactant alone. The $(12Ser)_2N12$:MO system shows an efficiency that increases gradually with increasing MO present, irrespective of the CR (+/-) used. However, the $(12Ser)_2COO12$:MO and $(12Ser)_2CON12$:MO systems behave differently: (i) they transfect HEK293eGFP cells more efficiently at high CR (+/-); (ii) at CR (+/-) = 10, increasing MO content leads to a moderate increase in transfection efficiency for the ester, but for the amide the variation seems to be non-monotonic with a peak at (1:1) gemini/MO molar ratio; (iii) at CR (+/-) = 5, increasing MO content has no significant effect in transfection efficiency, with the exception of the amide system, at (1:4) ratio.

These results clearly point to a complex dependence of the transfection ability on the composition of the systems, namely MO content and CR (+/-). Since the reasons behind this behavior could be, at least partially, related to the different structures that may form depending on the type of serine-derived gemini constituent, this hypothesis prompted us to a careful and detailed structural characterization of initial gemini/MO aggregates and derived lipoplexes for the three systems studied.

3.3. Characterization of the initial gemini/monoolein aggregates

The gemini surfactants studied in this work are soluble in water at 25 °C. However, they display a distinct self-aggregation behavior [12]. The amine derivative forms micelles as the first aggregate,

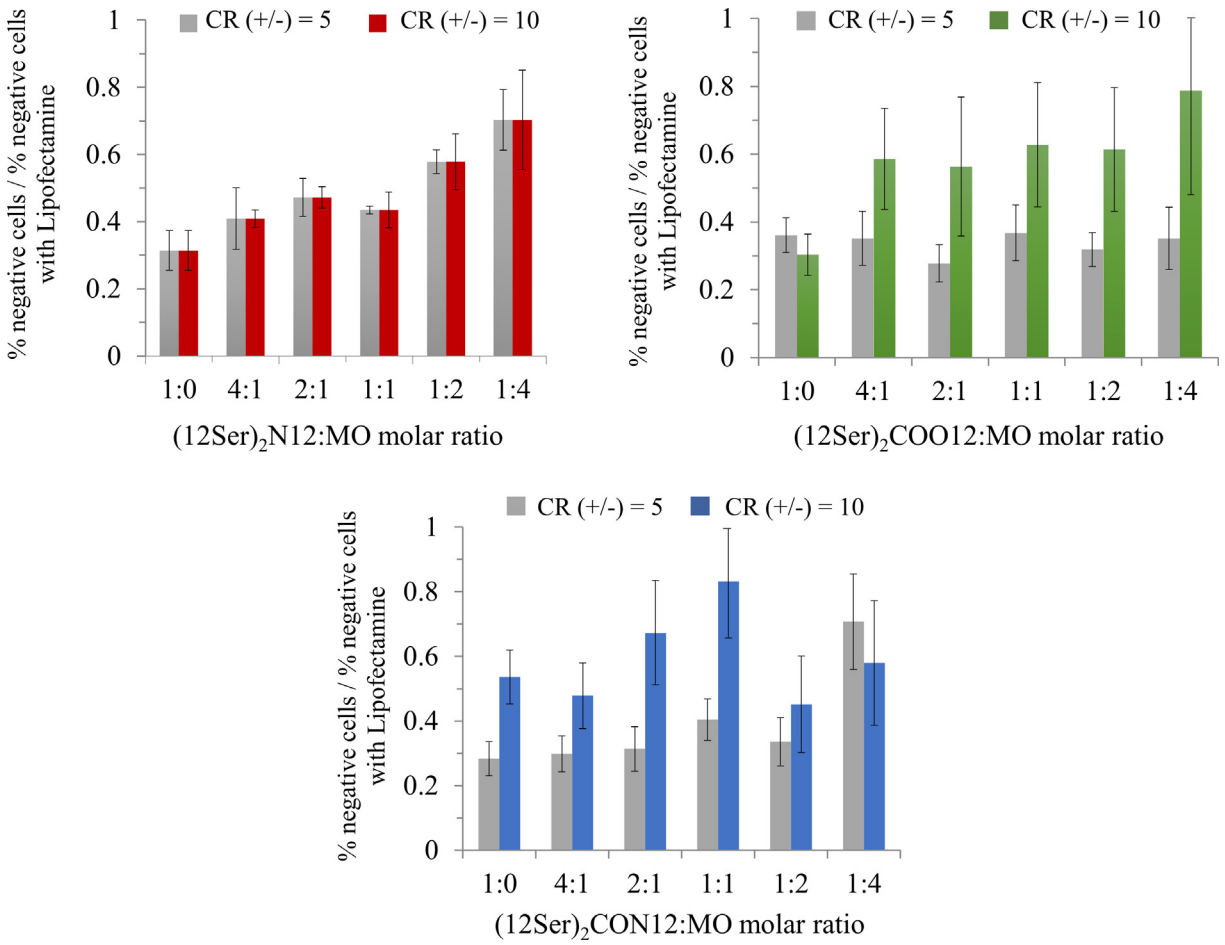

Fig. 2. Evaluation of eGFP gene silencing in HEK293eGFP cells, by flow cytometry, after 48 h of incubation with the different lipoplex systems tested, encapsulating anti-GFP siRNA at gemini-to-RNA charge ratio, CR (+/-), of 5 and 10, in comparison with transfection with Lipofectamine® RNAiMAX: top left, $(12Ser)_2N12$:MO system; top right, $(12Ser)_2COO12$:MO system; bottom, $(12Ser)_2CON12$:MO system. The molar ratio of cationic gemini surfactant to MO in the lipoplexes was varied as (1:0,) (4:1), (2:1), (1:1), (1:2) and (1:4).

while the amide and ester derivatives are bilayer-forming surfactants, forming large, polydisperse vesicles at low concentration. The incorporation of MO into these systems results in marked effects on particle size and polydispersity (DLS data), as can be followed in Table 2 (see also supplementary data, Fig. S2A).

Surfactant $(12Ser)_2N12$ alone in solution forms small micelles which is the result of having a critical packing parameter (as originally defined by Israelachvili et al) [60], P_s, of about 1/3 [12]. The $(12Ser)_2N12$:MO system presents a bimodal distribution between gemini:MO (4:1) up to (1:1), comprising a minor population of ca. 2.5 nm aggregates, consistent with micelles, and a major population of aggregates of $\langle D_H \rangle$ in the range 220–280 nm. Video-enhanced light microscopy (VELM) imaging (Fig. 3-c1) shows that this population consists of vesicles, which are observed for the entire range of $(12Ser)_2N12$:MO ratios covered. The observed irregular (and non-obvious) variation in frequency of the micellar population with MO content could be explained if the samples have not yet attained equilibrium composition. When there is excess MO, (1:2) and (1:4) ratios, the micelles seemingly vanish and only vesicles are present. An explanation for the observed effect of MO addition is the increase in the average packing parameter of the amphiphile system due to the bulky nature of MO, $P_s > 1$ [11], leading eventually to vesicles as the preferred aggregate structure ($P_s \approx 1$). Further evidence for the effect of MO in inducing bilayer phases, namely lamellar liquid crystals, is also found in phase scanning experiments of gemini/MO mixtures at high concentration (see supplementary data, Fig. S3).

Surfactants $(12Ser)_2COO12$ and $(12Ser)_2CON12$ dispersed alone in water form very large and polydisperse vesicles, as illustrated in Fig. 3-a2 for the amide derivative. For $(12Ser)_2COO12$, increasing content of MO leads to the formation of smaller and less polydisperse vesicles in general, with a changeover from a bimodal to monomodal distribution at (1:2) and (1:4) ratios (Table 2). For $(12Ser)_2CON12$, the trend is qualitatively similar, with two differences: monomodal size distributions appear between (2:1) and (1:2), and at maximum content of MO, (1:4), a bimodal distribution reappears, indicating that for the amide headgroup surfactant the packing interactions with MO are slightly different. Fig. 3-b2 and c2, for the amide:MO system at (1:1) and (1:4), illustrate that MO has indeed the effect of decreasing the mean size of the aggregates while maintaining the vesicle structure. We posit that the general reduction in vesicle size induced by MO in the ester and amide systems could be attributed to the fact that MO, having $P_s > 1$, and hence propensity to form negatively curved surfaces, may tend to reside preferentially in the inner monolayer of the vesicles, stabilizing aggregates of overall higher mean spontaneous curvature (i.e. lower $\langle D_H \rangle$). Phase scanning experiments further support that inclusion of MO preserves bilayer aggregates, as shown from the formation of lamellar liquid crystals (supplementary data, Fig. S3).

Table 2
Mean hydrodynamic diameter (<D_H> ± s.d.) and population frequency from DLS intensity distribution data, and zeta-potential (ζ-potential ± s.d.) values, for the aggregates formed by surfactants $(12Ser)_2N12$, $(12Ser)_2COO12$ and $(12Ser)_2CON12$ and MO at 1 mM total concentration and varying gemini:MO molar ratio (24 h after preparation).

gemini:MO molar ratio	Population A		Population B		
	<D_H>/nm	frequency/%	<D_H>/nm	frequency/%	ζ-potential/mV
$(12Ser)_2N12$:MO					
1:0	*		*		+63 ± 2
4:1	220 ± 17	88	2.4 ± 0.8	12	+59 ± 2
2:1	278 ± 53	66	2.6 ± 0.3	34	+59 ± 2
1:1	280 ± 27	84	2.5 ± 0.1	16	+54 ± 4
1:2	243 ± 58	100	–		+61 ± 2
1:4	401 ± 42	100	–		+61 ± 1
$(12Ser)_2COO12$:MO					
1:0	157 ± 40	12	1467 ± 73	88	+61 ± 3
4:1	197 ± 86	70	454 ± 15	30	+61 ± 2
2:1	226 ± 68	71	514 ± 53	29	+61 ± 2
1:1	146 ± 44	40	469 ± 54	60	+61 ± 2
1:2	245 ± 57	100	–	–	+65 ± 1
1:4	349 ± 49	100	–	–	+67 ± 2
$(12Ser)_2CON12$:MO					
1:0	179 ± 35	9	1147 ± 54	91	+67 ± 3
4:1	167 ± 12	58	989 ± 182	42	+64 ± 4
2:1	233 ± 92	100	–	–	+60 ± 2
1:1	216 ± 19	100	–	–	+60 ± 2
1:2	192 ± 2	100	–	–	+71 ± 1
1:4	132 ± 24	38	710 ± 104	62	+78 ± 1

*Not measurable (small micelles present).

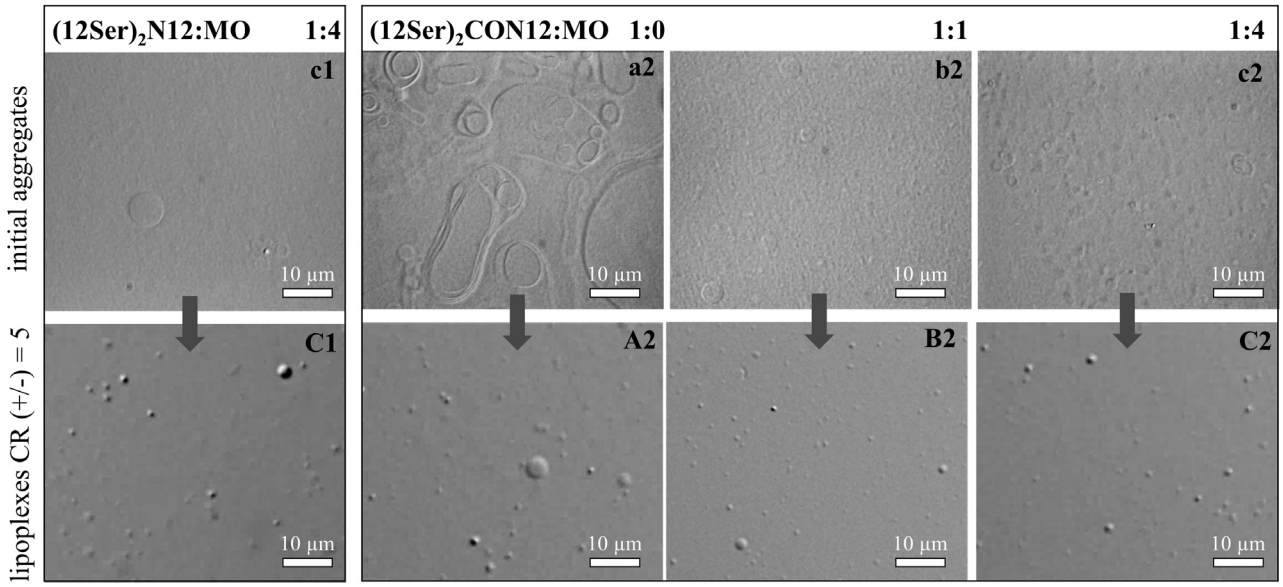

Fig. 3. Video-enhanced light microscopy imaging of the gemini/MO aggregates and derived lipoplexes, for the amine and amide gemini. The upper row micrographs, c1, a2, b2 and c2 show $(12Ser)_2N12$/MO and $(12Ser)_2CON12$/MO aggregates at total concentration of 5 mM, and varying gemini:MO molar ratio. In all cases, vesicle structures are observed with different size ranges. The lower row micrographs illustrate the lipoplexes obtained from the upper aggregates by adding siRNA at CR (+/-) = 5. Lipoplexes C1, A2, B2 and C2 are also presented below in Fig. 5, under cryo-TEM imaging, providing finer structural details.

Concerning the ζ-potential, its value is a key indicator of the kinetic stability of a colloidal dispersion. Dispersions with |ζ-potential| ≥ 40 mV have good or excellent stability while dispersions with |ζ-potential| < 30 mV have incipient stability and tend to flocculate or coagulate. All the studied systems present ζ-potential values above 54 mV (Table 2) indicating excellent colloidal stability for the aggregates. In basically all the systems, increasing MO content does not seem to have a significant effect on the surface charge of the aggregates, with the highest zeta potential achieved at gemini:MO (1:4) for the ester and amide systems. Taken altogether, these observations seem to be consistent with the hypothesis presented above on a preferential distribution of MO in the inner layer of vesicles.

Another significant observation is that the size of the mixed gemini/MO aggregates for all 3 systems tested remains essentially constant over a tested period of 60 days, irrespective of MO content (see supplementary data, Fig. S4). This indicates that MO inclusion does not hinder the stability of the aggregates over time (likely colloidal kinetic stability rather than thermodynamic stability), and could also be a consequence of the high values of zeta potential displayed.

3.4. Gemini/monoolein/siRNA lipoplex characterization

The study of lipoplex formation and structure by monitoring both size and ζ-potential provides important clues on the driving

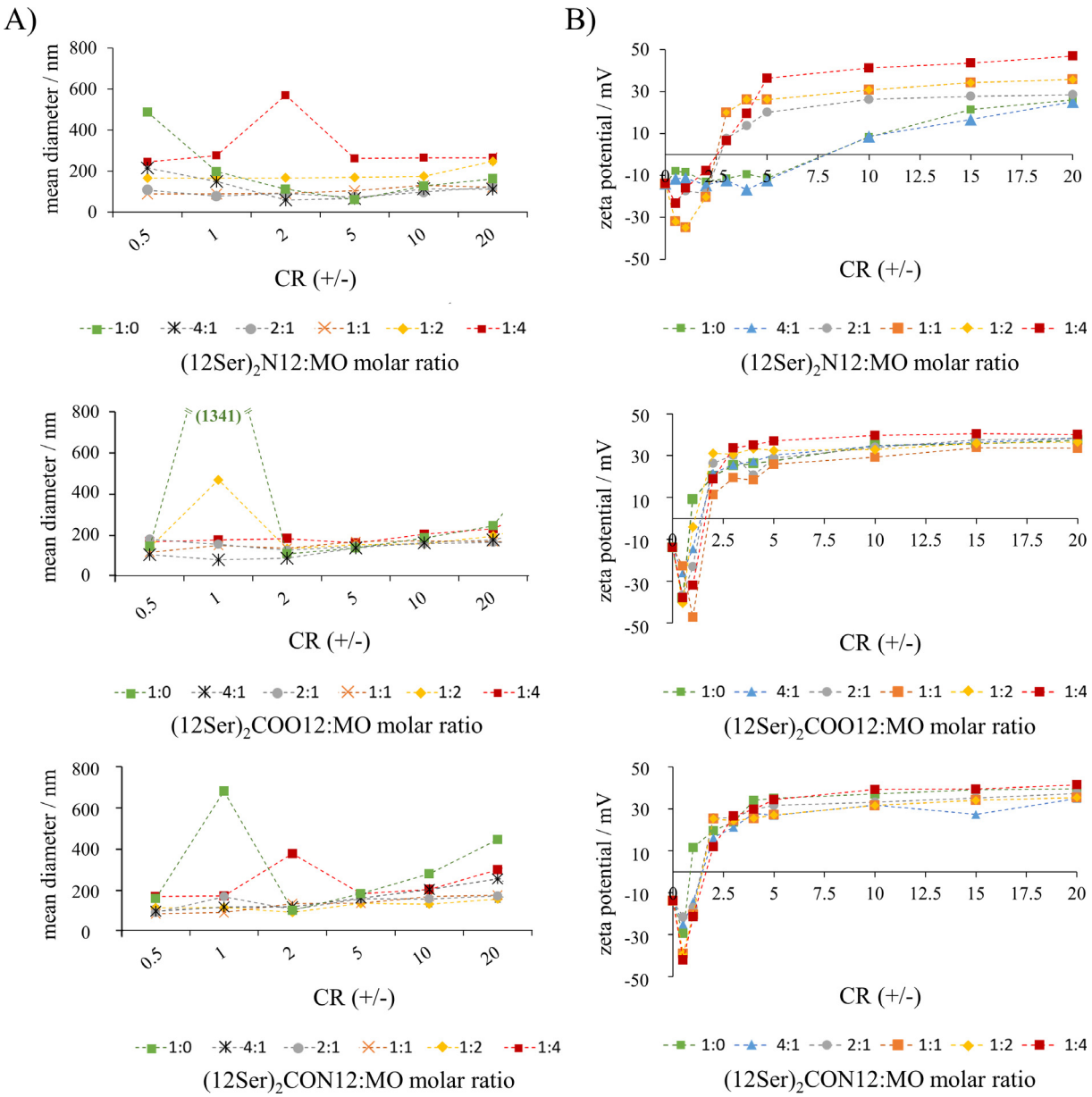

Fig. 4. (A) Mean diameter and (B) mean zeta potential for gemini/monoolein (MO)/siRNA lipoplexes as a function of the gemini/siRNA charge ratio, CR (+/-). The total gemini + MO concentration is 1 mM and the gemini/MO molar ratio in the lipoplexes varies between (1:0) to (1:4). For every point in the plots the error bar is ≤±5%.

forces during this process and possible implications for the transfection efficiency. Preliminary light microscopy studies, as illustrated in Fig. 3C1 and Fig. 3A2-C2 for CR (+/-) = 5, clearly showed that lipoplex formation is accompanied by a considerable reduction in size compared to the initial aggregates and suggest the presence of spheroidal vesicles aggregates in Brownian motion. A more in-depth characterization was performed by DLS, zeta potential measurements (Fig. 4) and cryo-TEM imaging (Fig. 5).

DLS size and zeta potential data are shown in Fig. 4(A) and (B), respectively, with CR (+/-) varying between 0.5 and 20 for each gemini/MO molar ratio (see also supplementary data, Fig. S2B). Fig. 4(A) shows that beyond the observed ζ-potential neutralization point, i.e. roughly for CR (+/-) ≥ 2, most of the lipoplexes have a mean diameter around 100–250 nm. It is also observed that around CR (+/-) = 1, lipoplexes have in some cases very large sizes (>500 nm), and that high CR (+/-) values (≥20) seem to also cause an increase in the size of the lipoplexes up to 600 nm.

The ζ-potential variation, Fig. 4(B), indicates that the negative charge of siRNA phosphates is neutralized by the increasing amount of cationic surfactant, as CR (+/-) increases. The $(12Ser)_2$-N12:MO lipoplexes display a somewhat complex profile, highly dependent on the MO content in the mixture. Lipoplexes with $(12Ser)_2$N12/MO molar ratio of (1:0) and (4:1), that is with low MO content, display very low ζ-potential until CR (+/-) ≈ 7.5, while the others reach the neutralization point at CR (+/-) ≈ 2.5, indicating that a higher MO content, (2:1) to (1:4), facilitates the process of siRNA complexation. In contrast, the $(12Ser)_2$COO12:MO and $(12Ser)_2$CON12:MO lipoplexes evolve from negatively to positively charged at CR (+/-) between 1 and 2, as could be reasonably expected. For CR (+/-) > 4 onwards, the ζ-potential levels off at ~ +40 mV, suggesting the stabilization of the lipoplex structure. Overall, at CR (+/-) = 5 and 10, all systems have formed stable lipoplexes, which were then deemed suitable for the cell transfection evaluation already shown above.

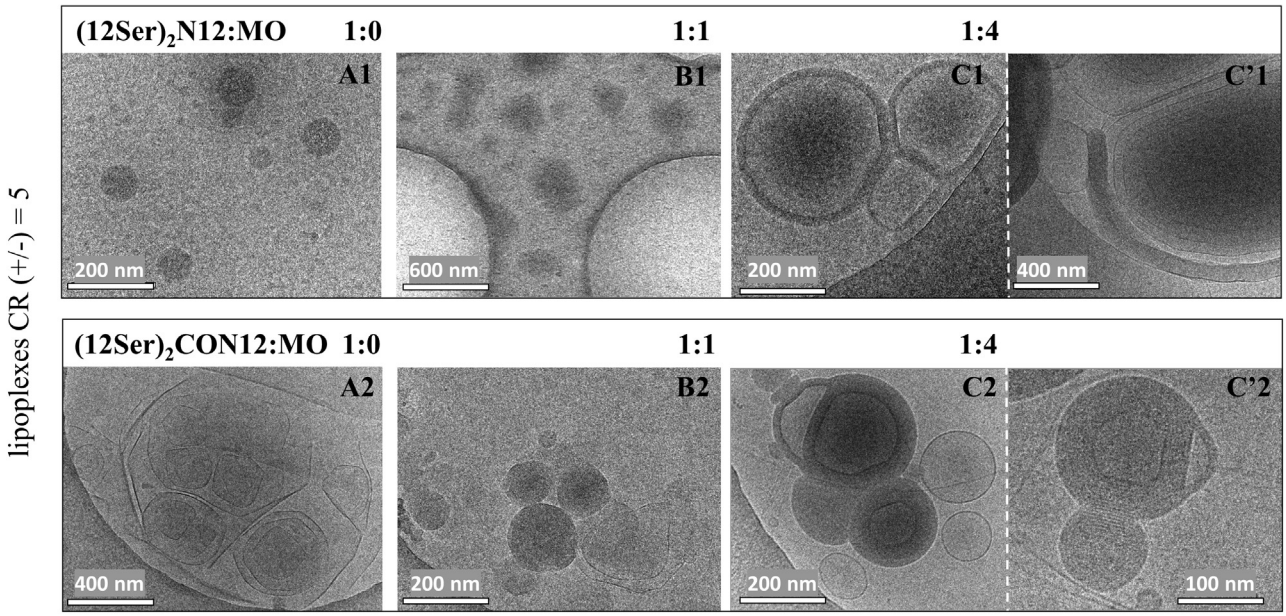

Fig. 5. Cryo-TEM imaging of the lipoplexes formed by the $(12Ser)_2$N12:MO (A1-C'1) and $(12Ser)_2$CON12:MO (A2-C'2) systems with fixed CR (+/-) = 5; lipoplexes have different gemini:MO molar ratios: (1:0) for A1 and A2; (1:1) for B1 and B2; (1:4) for C1, C'1, C2 and C'2.

In order to unveil with higher resolution the structure and morphology of the lipoplexes, cryo-TEM imaging was performed (Fig. 5). The lipoplexes with gemini:MO ratio of (1:0), (1:1) and (1:4), at fixed CR (+/-) = 5, were chosen, and the amine and amide surfactants were considered representative for these studies, given the similarity in structures typically observed between the amide and ester derivatives.

In Fig. 5A1, one observes for the neat amine derivative, $(12Ser)_2$-N12, 50–100 nm globular particles with high mass contrast, that could indicate the presence of incorporated siRNA. With a (1:1) MO content (Fig. 5B1), the particles seemingly increase in size (roughly 100–500 nm) and have a more irregular shape. At higher MO content (1:4), multilamellar structures, with clear sign of siRNA compaction in the bilayers (Fig. 5C1, dark rims), are observable. Moreover, some faceted bilayers are also clearly visible (Fig. 5C1′), with flat regions likely arising due to the polyanionic RNA binding onto the net cationic surface. These micrographs also show that the spheroidal particles seen by VELM in Fig. 3-C1, corresponding to the same sample as in Fig. 5C1, are indeed vesicular structures.

In contrast to the amine system, the neat amide $(12Ser)_2$CON12/siRNA lipoplex system, i.e. without MO present (Fig. 5A2), already shows the presence of vesicular structures, appearing faceted likely due to the nucleic acid binding. When MO is added in a (1:1) ratio (Fig. 5B2), 50–200 nm dark ill-defined nanoparticles are seen, similar to what is observed for the amine at this composition. At (1:4) ratio, 100–250 nm multilamellar vesicle structures are visible (Fig. 5C2), with some of them showing densely compacted bilayers due to siRNA binding (Fig. 5C2′), just as for the amine system. This type of structures correspond to typical multilamellar lipoplexes previously reported for various systems [61,62]. The imaging thus clearly shows that when present in high concentration, MO induces the formation of 100–200 nm densely packed lipoplexes with a multilamellar organization.

A study on the efficiency in siRNA complexation by the gemini/MO aggregates was also conducted, using a sensitive, specific nucleic acids stain (Ribogreen). This study allowed us to see some differences between the three gemini surfactants, as shown in Fig. 6. Aggregates containing $(12Ser)_2$N12 or $(12Ser)_2$COO12 become more effective in binding siRNA as the MO content increases. This effect seems to be more pronounced for the amine system. In contrast, the $(12Ser)_2$CON12:MO aggregates showed the same level of complexation efficiency irrespective of MO composition. Moreover, most systems reach maximal RNA complexation ability (80–90%) between CR (+/-) of 5 and 10—with few exceptions, such as $(12Ser)_2$N12:MO molar ratios (1:0), (4:1) and (2:1), and neat ester surfactant.

3.5. Outlook and comparisons with previous studies

A number of reviews published in recent years have comprehensively dealt with the use of gemini surfactants as transfections agents, alone or with helper lipids in assorted formulations [6,29,63]. The role of spacer length and nature, tail length and headgroup chemistry has been extensively studied, but direct comparisons looking for structure–function relationships can be obscured using different nucleic acid molecules, transfection strategies, cell lines and benchmarks. We will present the main trends herein observed, possible interpretations and comparisons with more directly related compounds and systems. The three serine-based gemini surfactants investigated here form mixed binary aggregates with monoolein that are able to efficiently transfect siRNA. The patterns presented by the different systems are somewhat complex, highlighting the role of headgroup chemical nature, when both tail length and spacer length are fixed.

While MO induces some cytotoxicity effects in these mixtures, contrarily to what we have observed with other cationic lipids [54,64]— namely with respect to the neat amine and ester derivatives, Table 1, less so with the amide one (possibly because this surfactant *per se* already has a low IC_{50} value)— it is also clear that MO content has a marked positive effect in the transfection ability (Fig. 2). This is observed for all the three systems and is in line with previous studies, where monovalent double-tailed surfactants were used (e.g. DOBAB/DODAC) [53,54]. Lipoplexes with cationic surfactant/RNA with CR (+/-) = 10 are particularly effective in the case of the ester and amide derivatives (ca. 80% with respect to Lipofectamine is attained), while for the amine derivative a CR (+/-) = 5 is sufficient to attain the best possible efficiency (ca. 70%). Moreover, for the ester and amide derivatives, a CR (+/-) = 5 is somewhat ineffective for transfection, irrespective of

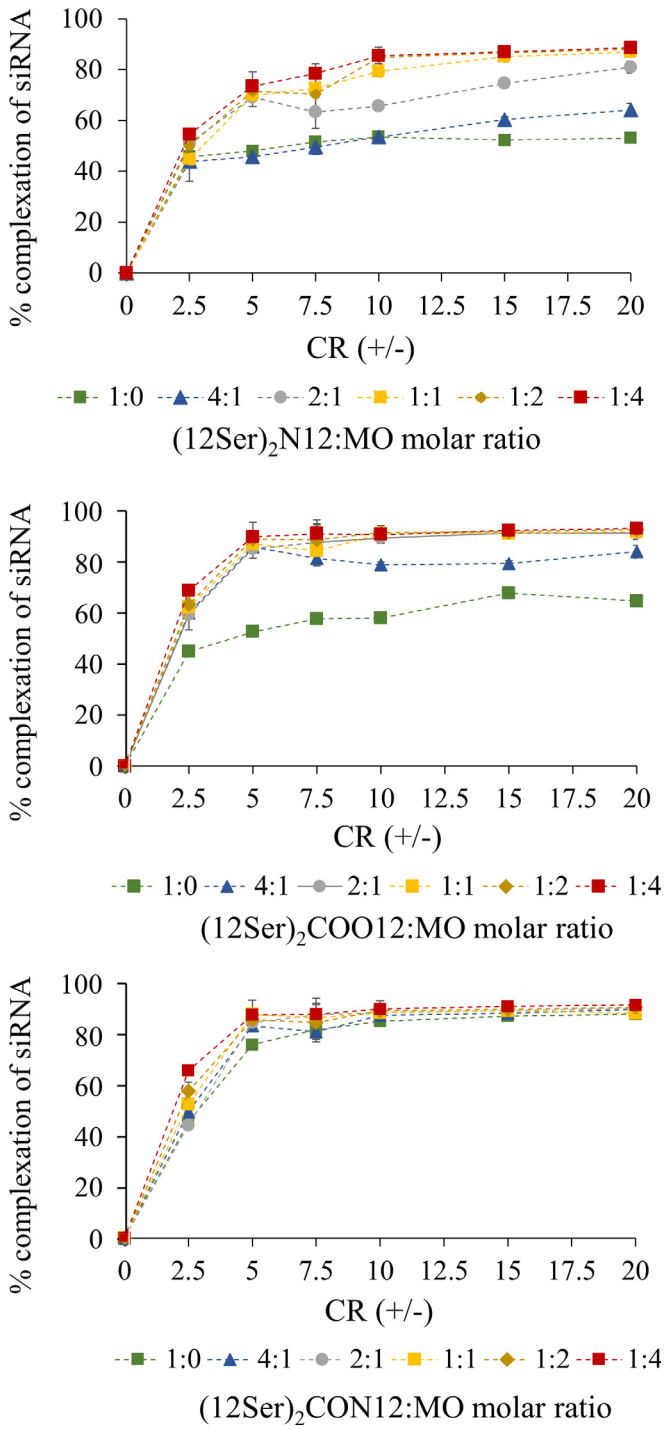

Fig. 6. Complexation of siRNA by gemini:MO aggregates (total MO + surfactant concentration is 1 mM) as a function of the CR (+/-).

the MO composition. Previously, we showed that MO has a fluidizing effect in liposomes constituted by DODAB (or DODAC) [54], affecting liposomal internalization and resulting transfection efficiency because of higher fusogenicity with the cell membrane. The results of the current study suggest that such influence by MO is observable in all three systems, although with differing relevance.

In an effort to shed light on these results, in terms of the relation between structure of the lipoplexes and transfection efficiency, we also found that (i) addition of MO leads to the formation of mixed vesicles in all three gemini surfactants, even in the case of the amine surfactant (which only forms micelles *per se*); (ii) in particular, for the amide and ester derivatives, the mixed vesicles become smaller and less polydisperse on increasing MO content; (iii) lipoplexes with high MO content, (1:4), have a multilamellar vesicle structure. In addition, the lipoplexes have sizes (<D_H>) in the range 100–250 nm, as shown consistently by DLS and cryo-TEM, and zeta potential values of about +40 mV.

Similar serine-based gemini surfactants have been used in our group in transfections studies, but with a five-carbon spacer and employing DOPE/cholesterol has helper lipid [36]. The surfactants have also shown to be efficient in DNA compaction and transfection. Namely the ester derivative $(12Ser)_2COO5$, reached 50% of transfected HeLa cells at low CR (+/-) = 1 and 2. When compared with Lipofectamine® 2000, serine-based surfactants transfected lower percentage of cells, but significantly they presented much lower cytotoxicity [36], a known limitation of this commercially available product. When comparing our current systems to lipoplexes formed by conventional bis-quaternary ammonium surfactants [65], the lipoplexes containing serine-derived surfactants present smaller sizes, compatible with intravenous administration, which quickens load delivery to cells and tissues, and improves drug bioavailability with low doses [66].

Summing up, the mixtures herein investigated constitute very interesting lipofection vectors as their cytotoxicity profile is very appropriate for biomedical use and offer good transfection efficiencies, which may be optimized in some conditions according to siRNA load and helper lipid content. Transfection efficiency is shown here in an experimental model with overexpression of eGFP, by modification of the wild type cell line, so it is legitimate to speculate that silencing a gene expressed in more physiological levels will probably be more effective.

4. Conclusions

Novel nanovectors were developed for siRNA delivery using serine-derived gemini surfactants — $(12Ser)_2N12$, amine derivative; $(12Ser)_2COO12$, ester derivative; and $(12Ser)_2CON12$, amide derivative — and monoolein (MO) as helper lipid. Bearing in mind the literature [6,29], our hypotheses were that the combination of the gemini amino acid-based structure of the cationic amphiphiles and a fusogenic lipid would result in innovative, effective transfection vectors, and that the gemini headgroup chemistry could also play a relevant role.

We found that the addition of MO to the gemini surfactants induces mixed vesicles, which typically become smaller and less polydisperse on increasing MO content. The siRNA lipoplexes with high MO content—gemini/MO molar ratio of (1:4)—have a multilamellar vesicle structure, and lipoplexes in general have mean diameters of 100–250 nm, suitable for both intravenous administration and effective transfection. Regarding RNA complexation, most systems reach maximal values (80–90%) for charge ratios (CR) (+/-) = 5–10. Although higher MO content typically favors complexation, systems containing amine and ester gemini are more dependent on lipid content for that than those with the amide gemini. A key finding is that most compositions of the three gemini/MO/siRNA systems lead to significant eGFP silencing, comparable to commercial standards, and without significant cytotoxicity. While the amine-gemini:MO systems become more transfection-efficient with increasing MO content irrespective of CR (+/-), the ester and amide systems' performance depends markedly on charge ratio, the best one being CR (+/-) = 10. For the latter systems, transfection efficiency either does not vary significantly (ester case) or varies non-monotonically (amide case) with the gemini:MO molar ratio. The final outcome is that the most effective systems are the amine-gemini:MO (1:4) at CR (+/-) = 5 or 10,

and the ester-gemini:MO (1:4) and amide-gemini:MO (1:1) both at CR (+/-) = 10. The aggregate concentration for gene silencing does not induce significant toxicity on human (HEK 293 T) cells.

Overall, it is shown that gemini serine-based surfactants and monoolein combine indeed to yield robust and effective vectors for siRNA transfection. The amine-gemini:MO systems are particularly promising due to lower cytotoxicity and transfection efficiency less dependent on charge ratio, yet further optimization could be performed for all three systems. Our findings are thus a contribution for the search of ever more efficient and safe non-viral vectors for gene delivery.

CRediT authorship contribution statement

Catarina Costa: Investigation, Formal analysis, Validation, Writing - original draft. **Isabel S. Oliveira:** Investigation, Formal analysis, Validation, Writing - original draft. **João P.N. Silva:** Investigation, Formal analysis. **Sandra G. Silva:** Investigation, Formal analysis, Validation, Writing - original draft. **Cláudia Botelho:** Investigation, Formal analysis. **M. Luísa C. do Vale:** Methodology, Resources, Supervision, Writing - review & editing. **Maria Elisabete C.D. Real Oliveira:** Methodology, Resources, Supervision. **Andreia C. Gomes:** Conceptualization, Resources, Supervision, Funding acquisition, Writing - review & editing. **Eduardo F. Marques:** Conceptualization, Resources, Supervision, Funding acquisition, Writing - review & editing.

Declaration of Competing Interest

The authors declare that they have no known competing financial interests or personal relationships that could have appeared to influence the work reported in this paper.

Acknowledgements

The authors acknowledge Fundação para a Ciência e a Tecnologia (FCT) for financial support through projects UIDB/00081/2020 and UIDB/50006/2020. This work was supported by the "Contrato-Programa" UIDB/04050/2020 funded by national funds through the FCT I.P. Dr. Marisa Passos is gratefully acknowledged for help with the statistical analysis of cytotoxicity data. Funding by the CCDR-N/NORTE2020/Portugal2020 through project DESign-BIOtechHealth (ref. Norte-01-0145-FEDER-000024) is also acknowledged. I. S. Oliveira and S.G. Silva also acknowledge financial support from FCT through PhD grant SFRH/BD/108629/2015 and Individual Call to Scientific Employment Stimulus - CEEC Individual grant CEECIND/01932/2017, respectively.

Appendix A. Supplementary material

Supplementary data to this article can be found online at https://doi.org/10.1016/j.jcis.2020.09.077.

References

[1] H.Y. Wang, Y.F. Jiang, H.G. Peng, Y.Z. Chen, P.Z. Zhu, Y.Z. Huang, Recent progress in microRNA delivery for cancer therapy by non-viral synthetic vectors, Adv. Drug Deliv. Rev. 81 (2015) 142–160.
[2] M. Ramamoorth, A. Narvekar, Non Viral Vectors in Gene Therapy- An Overview, J. Clin. Diagn. Res. 9 (2015) GE1-GE6.
[3] M.K. Riley, W. Vermerris, Recent Advances in Nanomaterials for Gene Delivery-A Review, Nanomaterials 7 (2017).
[4] E. Fattal, A. Bochot, State of the art and perspectives for the delivery of antisense oligonucleotides and siRNA by polymeric nanocarriers, Int. J. Pharm. 364 (2008) 237–248.
[5] F. Liu, C.F. Wang, Y.T. Gao, X. Li, F. Tian, Y.T. Zhang, M.Y. Fu, P.F. Li, Y.L. Wang, F. Wang, Current Transport Systems and Clinical Applications for Small Interfering RNA (siRNA) Drugs, Mol. Diagn. Ther. 22 (2018) 551–569.
[6] M. Damen, A.J.J. Groenen, S.F.M. van Dongen, R.J.M. Nolte, B.J. Scholte, M.C. Feiters, Transfection by cationic gemini lipids and surfactants, Medchemcomm. 9 (2018) 1404–1425.
[7] Y.K. Oh, T.G. Park, siRNA delivery systems for cancer treatment, Adv. Drug Deliv. Rev. 61 (2009) 850–862.
[8] Y.-C. Tseng, S. Mozumdar, L. Huang, Lipid-based systemic delivery of siRNA, Adv. Drug Deliv. Rev. 61 (2009) 721–731.
[9] C.-F. Xu, J. Wang, Delivery systems for siRNA drug development in cancer therapy, Asian J. Pharm. Sci. 10 (2015) 1–12.
[10] L. Han, C. Tang, C. Yin, Enhanced antitumor efficacies of multifunctional nanocomplexes through knocking down the barriers for siRNA delivery, Biomaterials 44 (2015) 111–121.
[11] I.M.S.C. Oliveira, J.P.N. Silva, E. Feitosa, E.F. Marques, E.M.S. Castanheira, M.E.C. D. Real Oliveira, Aggregation behavior of aqueous dioctadecyldimethylammonium bromide/monoolein mixtures: A multitechnique investigation on the influence of composition and temperature, J. Colloid Interface Sci. 374 (2012) 206–217.
[12] S.G. Silva, I.S. Oliveira, M.L.C. do Vale, E.F. Marques, Serine-based gemini surfactants with different spacer linkages: from self-assembly to DNA compaction, Soft Matter 10 (2014) 9352–9361.
[13] G. Shim, M.-G. Kim, J.Y. Park, Y.-K. Oh, Application of cationic liposomes for delivery of nucleic acids, Asian J. Pharm. Sci. 8 (2013) 72–80.
[14] L.K. Müller, K. Landfester, Natural liposomes and synthetic polymeric structures for biomedical applications, Biochem. Biophys. Res. Commun. 468 (2015) 411–418.
[15] I. Eş, M.T. Ok, X.E. Puentes-Martinez, M.A.S. de Toledo, M.T. de Pinho Favaro, L. P. Cavalcanti, A. Cassago, R.V. Portugal, A.R. Azzoni, L.G. de la Torre, Evaluation of siRNA and cationic liposomes complexes as a model for in vitro siRNA delivery to cancer cells, Colloids Surf., A Physicochem. Eng. Asp. 555 (2018) 280–289.
[16] R. Zana, Dimeric (Gemini) Surfactants: Effect of the Spacer Group on the Association Behavior in Aqueous Solution, J. Colloid Interface Sci. 248 (2002) 203–220.
[17] F.M. Menger, J.S. Keiper, Gemini surfactants, Angew. Chem. Int. Edit. 39 (2000) 1907–1920.
[18] B. Abreu, J. Rocha, R.M.F. Fernandes, O. Regev, I. Furo, E.F. Marques, Gemini surfactants as efficient dispersants of multiwalled carbon nanotubes: Interplay of molecular parameters on nanotube dispersibility and debundling, J. Colloid Interface Sci. 547 (2019) 69–77.
[19] L. Mivehi, R. Bordes, K. Holmberg, Adsorption of Cationic Gemini Surfactants at Solid Surfaces Studied by QCM-D and SPR: Effect of the Rigidity of the Spacer, Langmuir 27 (2011) 7549–7557.
[20] R. Zana, Dimeric and oligomeric surfactants. Behavior at interfaces and in aqueous solution: a review, Adv. Colloid Interface Sci. 97 (2002) 205–253.
[21] S.D. Wettig, X.F. Li, R.E. Verrall, Thermodynamic and aggregation properties of gemini surfactants with ethoxylated spacers in aqueous solution, Langmuir 19 (2003) 3666–3670.
[22] Y. Han, Y. Wang, Aggregation behavior of gemini surfactants and their interaction with macromolecules in aqueous solution, Phys. Chem. Chem. Phys. 13 (2011) 1939–1956.
[23] G. Ronsin, C. Perrin, P. Guedat, A. Kremer, P. Camilleri, A.J. Kirby, Novel spermine-based cationic gemini surfactants for gene delivery, Chem. Commun. 2234–2235 (2001).
[24] C. McGregor, C. Perrin, M. Monck, P. Camilleri, A.J. Kirby, Rational Approaches to the Design of Cationic Gemini Surfactants for Gene Delivery, J. Am. Chem. Soc. 123 (2001) 6215–6220.
[25] D. Zhi, S. Zhang, S. Cui, Y. Zhao, Y. Wang, D. Zhao, The Headgroup Evolution of Cationic Lipids for Gene Delivery, Bioconjug. Chem. 24 (2013) 487–519.
[26] P. Camilleri, A. Kremer, A.J. Edwards, K.H. Jennings, O. Jenkins, I. Marshall, C. McGregor, W. Neville, S.Q. Rice, R.J. Smith, M.J. Wilkinson, A.J. Kirby, A novel class of cationic surfactants showing efficient gene transfection properties, Chem. Commun. 1253–1254 (2000).
[27] Z. Pietralik, J.R. Kumita, C.M. Dobson, M. Kozak, The influence of novel gemini surfactants containing cycloalkyl side-chains on the structural phases of DNA in solution, Colloids Surf. B Biointerfaces 131 (2015) 83–92.
[28] T. Ahmed, A.O. Kamel, S.D. Wettig, Interactions between DNA and gemini surfactant: impact on gene therapy: part II, Nanomedicine 11 (2016) 403–420.
[29] T. Ahmed, A.O. Kamel, S.D. Wettig, Interactions between DNA and gemini surfactant: impact on gene therapy: part I, Nanomedicine 11 (2016) 289–306.
[30] E. Fisicaro, C. Compari, F. Bacciottini, L. Contardi, E. Pongiluppi, N. Barbero, G. Viscardi, P. Quagliotto, G. Donofrio, M.P. Krafft, Nonviral gene-delivery by highly fluorinated gemini bispyridinium surfactant-based DNA nanoparticles, J. Colloid Interface Sci. 487 (2017) 182–191.
[31] B. Sarrion, E. Bernal, V.I. Martin, M. Lopez-Lopez, P. Lopez-Cornejo, M. Garcia-Calderon, M.L. Moya, Binding of 12-s-12 dimeric surfactants to calf thymus DNA: Evaluation of the spacer length influence, Colloids Surf. B Biointerfaces 144 (2016) 311–318.
[32] M. Martinez-Negro, A.L. Barran-Berdon, C. Aicart-Ramos, M.L. Moya, C.T. de Ilarduya, E. Aicart, E. Junquera, Transfection of plasmid DNA by nanocarriers containing a gemini cationic lipid with an aromatic spacer or its monomeric counterpart, Colloids Surf. B Biointerfaces 161 (2018) 519–527.
[33] D.R. Acosta-Martinez, E. Rodriguez-Velazquez, F. Araiza-Verduzco, P. Taboada, G. Prieto, I.A. Rivero, G. Pina-Luis, M. Alatorre-Meda, Bis-quaternary ammonium gemini surfactants for gene therapy: Effects of the spacer hydrophobicity on the DNA complexation and biological activity, Colloids Surf. B Biointerfaces 189 (2020).

[34] A. Colomer, A. Pinazo, M.A. Manresa, M.P. Vinardell, M. Mitjans, M.R. Infante, L. Pérez, Cationic Surfactants Derived from Lysine: Effects of Their Structure and Charge Type on Antimicrobial and Hemolytic Activities, J. Med. Chem. 54 (2011) 989–1002.
[35] L. Pérez, A. Pinazo, R. Pons, M. Infante, Gemini surfactants from natural amino acids, Adv. Colloid Interfac. Sci. 205 (2014) 134–155.
[36] A.M. Cardoso, C.M. Morais, A.R. Cruz, S.G. Silva, M.L. do Vale, E.F. Marques, M.C. P. de Lima, A.S. Jurado, New serine-derived gemini surfactants as gene delivery systems, Eur. J. Pharm. Biopharm. 89 (2015) 347–356.
[37] J.D. Wolf, M. Kurpiers, R.A. Baus, R.X. Gotz, J. Griesser, B. Matuszczak, A. Bernkop-Schnurch, Characterization of an amino acid based biodegradable surfactant facilitating the incorporation of DNA into lipophilic delivery systems, J. Colloid Interface Sci. 566 (2020) 234–241.
[38] M.R. Infante, L. Pérez, M.C. Morán, R. Pons, M. Mitjans, M.P. Vinardell, M.T. Garcia, A. Pinazo, Biocompatible surfactants from renewable hydrophiles, Eur. J. Lipid Sci. Technol. 112 (2010) 110–121.
[39] M.T. Calejo, A.-L. Kjøniksen, A. Pinazo, L. Pérez, A.M.S. Cardoso, M.C. Pedroso de Lima, A.S. Jurado, S.A. Sande, B. Nyström, Thermoresponsive hydrogels with low toxicity from mixtures of ethyl(hydroxyethyl) cellulose and arginine-based surfactants, Int. J. Pharm. 436 (2012) 454–462.
[40] P. Yang, J. Singh, S. Wettig, M. Foldvari, R.E. Verrall, I. Badea, Enhanced gene expression in epithelial cells transfected with amino acid-substituted gemini nanoparticles, Eur. J. Pharm. Biopharm. 75 (2010) 311–320.
[41] Y. Zheng, Y.J. Guo, Y.T. Li, Y. Wu, L.H. Zhang, Z.J. Yang, A novel gemini-like cationic lipid for the efficient delivery of siRNA, New J. Chem. 38 (2014) 4952–4962.
[42] M. Castro, D. Griffiths, A. Patel, N. Pattrick, C. Kitson, M. Ladlow, Effect of chain length on transfection properties of spermine-based gemini surfactants, Org. Biomol. Chem. 2 (2004) 2814–2820.
[43] R.O. Brito, E.F. Marques, S.G. Silva, M.L. do Vale, P. Gomes, M.J. Araújo, J.E. Rodriguez-Borges, M.R. Infante, M.T. Garcia, I. Ribosa, M.P. Vinardell, M. Mitjans, Physicochemical and toxicological properties of novel amino acid-based amphiphiles and their spontaneously formed catanionic vesicles, Colloids Surf. B Biointerfaces 72 (2009) 80–87.
[44] S.G. Silva, J.E. Rodríguez-Borges, E.F. Marques, M.L.C. do Vale, Towards novel efficient monomeric surfactants based on serine, tyrosine and 4-hydroxyproline: synthesis and micellization properties, Tetrahedron 65 (2009) 4156–4164.
[45] R.O. Brito, S.G. Silva, R.M.F. Fernandes, E.F. Marques, J. Enrique-Borges, M.L.C. do Vale, Enhanced interfacial properties of novel amino acid-derived surfactants: Effects of headgroup chemistry and of alkyl chain length and unsaturation, Colloids Surf. B Biointerfaces 86 (2011) 65–70.
[46] S.G. Silva, C. Alves, A.M.S. Cardoso, A.S. Jurado, M.C. Pedroso de Lima, M.L.C. Vale, E.F. Marques, Synthesis of Gemini Surfactants and Evaluation of Their Interfacial and Cytotoxic Properties: Exploring the Multifunctionality of Serine as Headgroup, Eur. J. Org. Chem. 2013 (2013) 1758–1769.
[47] S.G. Silva, R.F. Fernandes, E.F. Marques, M.L.C. do Vale, Serine-Based Bis-quat Gemini Surfactants: Synthesis and Micellization Properties, Eur. J. Org. Chem. (2012) 345–352.
[48] C. Bombelli, L. Giansanti, P. Luciani, G. Mancini, Gemini Surfactant Based Carriers in Gene and Drug Delivery, Curr. Med. Chem. 16 (2009) 171–183.
[49] S.W. Hui, M. Langner, Y.L. Zhao, P. Ross, E. Hurley, K. Chan, The role of helper lipids in cationic liposome-mediated gene transfer, Biophys. J. 71 (1996) 590–599.
[50] I.S. Zuhorn, U. Bakowsky, E. Polushkin, W.H. Visser, M.C.A. Stuart, J.B.F.N. Engberts, D. Hoekstra, Nonbilayer phase of lipoplex-membrane mixture determines endosomal escape of genetic cargo and transfection efficiency, Mol. Ther. 11 (2005) 801–810.
[51] J.P.N. Silva, P.J.G. Coutinho, M.E.C.D.R. Oliveira, Characterization of Monoolein-Based Lipoplexes Using Fluorescence Spectroscopy, J. Fluoresc. 18 (2008) 555–562.
[52] A.C.N. Oliveira, J.P. Neves Silva, P.J.G. Coutinho, A.A. Gomes, O.P. Coutinho, M.E. C.D. Real Oliveira, Monoolein as helper lipid for non-viral transfection in mammals, J. Control. Release 148 (2010) e91–e92.
[53] J.P.N. Silva, A.C.N. Oliveira, M.P.P.A. Casal, A.C. Gomes, P.J.G. Coutinho, O.P. Coutinho, M.E.C.D.R. Oliveira, DODAB:monoolein-based lipoplexes as non-viral vectors for transfection of mammalian cells, Biochim. Biophys. Acta - Biomembranes 1808 (2011) 2440–2449.
[54] A.C.N. Oliveira, T.F. Martens, K. Raemdonck, R.D. Adati, E. Feitosa, C. Botelho, A. C. Gomes, K. Braeckmans, M.E.C.D. Real Oliveira, Dioctadecyldimethylammonium: Monoolein Nanocarriers for Efficient in Vitro Gene Silencing, ACS Appl. Mater. Interfaces 6 (2014) 6977–6989.
[55] J. Briggs, H. Chung, M. Caffrey, The temperature-composition phase diagram and mesophase structure characterization of the monoolein/water system, J. Phys. II (6) (1996) 723–751.
[56] B. Geil, T. Feiweier, E.M. Pospiech, J. Eisenblätter, F. Fujara, R. Winter, Relating structure and translational dynamics in aqueous dispersions of monoolein, Chem. Phys. Lipids 106 (2000) 115–126.
[57] V. Luzzati, Biological significance of lipid polymorphism: the cubic phases, Curr. Opin. Struct. Biol. 7 (1997) 661–668.
[58] S. Bhattacharjee, DLS and zeta potential - What they are and what they are not?, J. Control. Release 235 (2016) 337–351.
[59] P.A. Hassan, S. Rana, G. Verma, Making Sense of Brownian Motion: Colloid Characterization by Dynamic Light Scattering, Langmuir 31 (2015) 3–12.
[60] J.N. Israelachvili, D.J. Mitchell, B.W. Ninham, Theory of self-assembly of hydrocarbon amphiphiles into micelles and bilayers, J. Chem. Soc. Faraday Trans. 72 (1976) 1525–1568.
[61] P.C. Bell, M. Bergsma, I.P. Dolbnya, W. Bras, M.C.A. Stuart, A.E. Rowan, M.C. Feiters, J.B.F.N. Engberts, Transfection Mediated by Gemini Surfactants: Engineered Escape from the Endosomal Compartment, J. Am. Chem. Soc. 125 (2003) 1551–1558.
[62] N. Dan, D. Danino, Structure and kinetics of lipid–nucleic acid complexes, Adv. Colloid Interface Sci. 205 (2014) 230–239.
[63] E. Junquera, E. Aicart, Recent progress in gene therapy to deliver nucleic acids with multivalent cationic vectors, Adv. Colloid Interface Sci. 233 (2016) 161–175.
[64] A.C.N. Oliveira, M.P. Sarria, P. Moreira, J. Fernandes, L. Castro, I. Lopes, M. Corte-Real, A. Cavaco-Paulo, M. Oliveira, A.C. Gomes, Counter ions and constituents combination affect DODAX: MO nanocarriers toxicity in vitro and in vivo, Toxicol. Res. 5 (2016) 1244–1255.
[65] A.M. Cardoso, C.M. Morais, S.G. Silva, E.F. Marques, M.C.P. de Lima, M.A.S. Jurado, Bis-quaternary gemini surfactants as components of nonviral gene delivery systems: A comprehensive study from physicochemical properties to membrane interactions, Int. J. Pharm. 474 (2014) 57–69.
[66] D. Chenthamara, S. Subramaniam, S.G. Ramakrishnan, S. Krishnaswamy, M.M. Essa, F.-H. Lin, M.W. Qoronfleh, Therapeutic efficacy of nanoparticles and routes of administration, Biomat. Res. 23 (2019) 20.